Influence of heating conditions and initial thickness on the effectiveness of thin intumescent coatings

Andrea Lucherini[a*], Juan P. Hidalgo[a], Jose L. Torero[b], Cristian Maluk[a]

[a]School of Civil Engineering, The University of Queensland, Australia

[b]Department of Civil, Environmental & Geomatic Engineering, University College London, UK

*Corresponding author: a.lucherini@uq.edu.au

Highlights:

- Experimental methodology to gauge the thermo-physical response of intumescent coatings.
- The swelling and the swelled thickness govern the effectiveness of intumescent coatings.
- Heating conditions govern the swelling rate of intumescent coatings.
- Applied initial thickness governs the maximum swelled thickness.
- Empirical correlations for swelling rate and maximum swelled thickness.

Abstract:

The study presented herein shows an experimental methodology aimed at analysing the effectiveness of intumescent coatings through a detailed characterisation of their thermo-physical response for a range of heating conditions and applied initial dry film thickness (DFT). Steel plates coated with a commercial solvent-based thin intumescent coating were exposed to well-defined and highly-repeatable heating conditions in accordance with the H-TRIS test method. Experimental results emphasise that the swelling process and the resulting swelled thickness govern the thermo-physical response of intumescent coatings, thus their effectiveness. During swelling, the coated steel asymptotically tends to the temperature range 300-350°C, regardless of the heating condition or the initial DFT. Thermo-Gravimetric Analysis (TGA) experiments demonstrate that the coating undergoes the swelling reaction at this temperature range. Once the swelling process is completed, the steel temperature increases above 350°C. The steel temperature acts as an indicator of the swelling process, as the reaction occurs in the proximity to the steel-coating interface. The intumescent coating swells and insulates the steel substrate by displacing the already-swelled coating towards the direction of the source of heat. Aiming at predicting the swelling of intumescent coatings, empirical correlations are derived: the swelling rate is governed by the heating conditions and the maximum swelled thickness is governed by the applied initial DFT.

Keywords: intumescent coatings; steel structures; swelling; heating conditions; initial thickness; heat transfer; fire testing; H-TRIS; fire safety.

1. Introduction and background

Steel structures represent a mainstream building structural system in the modern construction industry. As structural systems, the integrity and stability of steel structures may be compromised during and after a fire due to loss of strength and stiffness, as well as thermally induced forces and displacements [1]. The application of thermal barriers characterised by low thermal diffusivity is the traditional solution to reduce the temperature increase of the load-bearing structure during a

fire [2]. Conventional solutions, such as gypsum plasterboards or cementitious spray-on systems, are usually deemed to be relatively inexpensive and easy to apply, but aesthetically unpleasant and an undesirable choice in varied applications, such as slender structures with visible steelwork.

The unique advantages of intumescent coatings, such as the low impact on the attractive architectural appearance of bare steel structures and flexibility for both on- and off-site applications, have fostered their success and extensive use all over the world [3-5]. Consequently, intumescent coatings currently represent a dominant fire safety solution for protecting load-bearing structural steel systems. Upon sufficient heating, intumescent coatings swell to form a low-density and highly-insulating porous media that prevents the steel elements from reaching high temperatures [6]. The formulation of thin intumescent coatings for the built environment is typically waterborne or solvent-based. They are usually applied to a target Dry Film Thickness (DFT) of a few millimetres and, when exposed to heat, they can swell up to 100 times their initial thickness [5, 7].

Within the structural and fire safety engineering practice, the insulating capacity of intumescent coatings is commonly assessed using two simplified engineering design methods based on exposure to the standard temperature-time fire curve in a furnace [8-9]. These methods are developed based on experimentally measured temperatures of coated steel samples tested in a standard fire resistance test. The first method consists of creating *tabulated fire ratings*, where manufacturers offer design tables that list the minimum DFTs required to ensure a certain level of fire protection (i.e. the steel temperature remains below a certain predefined critical value in the standard fire resistance furnace test). Alternatively, the European *effective thermal conductivity method* can be used to simulate the heat transfer from the fire into the steel using a lumped capacitance approximation of the transient heat conduction problem [9]. This method assumes that the intumescent coating does not expand, but it experiences a transient change of its thermal conductivity. The resulting temperature-dependent effective thermal conductivity of the intumescent coating estimates an equivalent thermal barrier to the protected structure and this method implicitly assumes that the thermo-physical properties of the intumescent coating only depend on the temperature [10]. However, intumescent coatings are chemically reactive materials and numerous researchers have emphasised the influence of the heating conditions on the intumescent process and the overall insulating effectiveness [6, 11-16]. In particular, slow-growing fires or low heating regimes may have a negative impact on the insulating performance of intumescent coatings by causing incomplete swelling or even melting and delamination [6, 14, 15].

As a consequence, the current procedures do not represent a comprehensive design practice to ensure the fire safety of steel structures. They do not fully assess the effectiveness of intumescent coatings through a detailed characterisation of the heat transfer within the swelling coating. Most importantly, these simplified engineering methods simulate the temperature evolution of coated steel samples in furnaces exposed to a single heating scenario, not addressing the whole range of potential heating regimes occurring in a fire. In a world moving towards performance-based engineering solutions, there is a need for explicitly understanding how different factors may influence the effectiveness of intumescent coatings, e.g. heating conditions and applied initial thickness. By obtaining this scientific and practical knowledge, it will be possible to formulate and validate models able to produce realistic and reliable predictions for the fire-safe design of steel structures [10].

The available literature presents limited research studies that have looked at assessing the effectiveness of intumescent coatings through their thermo-physical response [10]. This progress is commonly inhibited by inadequate testing methodologies and experimental setups. In particular, standard fire resistance tests in furnaces have been questioned due to the poor repeatability and the uncertain thermal boundary conditions imposed on test samples [17-18]. In addition, the closed environment of standard furnaces does not allow for accurate visual inspection of test samples during the heating exposure, a key aspect to comprehend the thermo-physical response of intumescent coatings [19]. A few researchers have proposed various approaches and methodologies to analyse the heat transfer within intumescent coatings by placing in-depth thermocouples within intumescent coatings [20-22]. However, this methodology has been adopted in only a few cases because of the experimental difficulties related to gauging accurate measurements of the in-depth temperature distributions without disturbing the swelling process.

The study presented herein shows an experimental methodology aimed at analysing the effectiveness of intumescent coatings through a detailed characterisation of their thermo-physical response. In particular, the influences of different heating conditions and the applied initial thickness were investigated. Steel plates coated with a commercial solvent-based thin intumescent coating were exposed to well-defined and highly-repeatable heating conditions using the Heat-Transfer Rate Inducing System (H-TRIS) test method. Test samples were thoroughly instrumented in order to measure the real-time swelled coating thickness, the exposed surface temperature, the steel temperature and the in-depth transient temperature profile within the intumescent coating.

2. Material and methods

2.1 Experimental methodology

The experimental methodology was chosen in order to have direct control and quantification of the thermal boundary conditions imposed on the test samples, ensuring high repeatability between experiments at low economic and temporal costs. The Heat-Transfer Rate Inducing System (H-TRIS) offers these advantages over conventional testing, therefore it was selected as the appropriate experimental methodology [18]. H-TRIS accurately controls the relative position between the target exposed surface of the test sample and the surface of an array of radiant panels, moving on a computer-controlled linear motion system (Fig. 1). In this way, H-TRIS is able to impose a well-

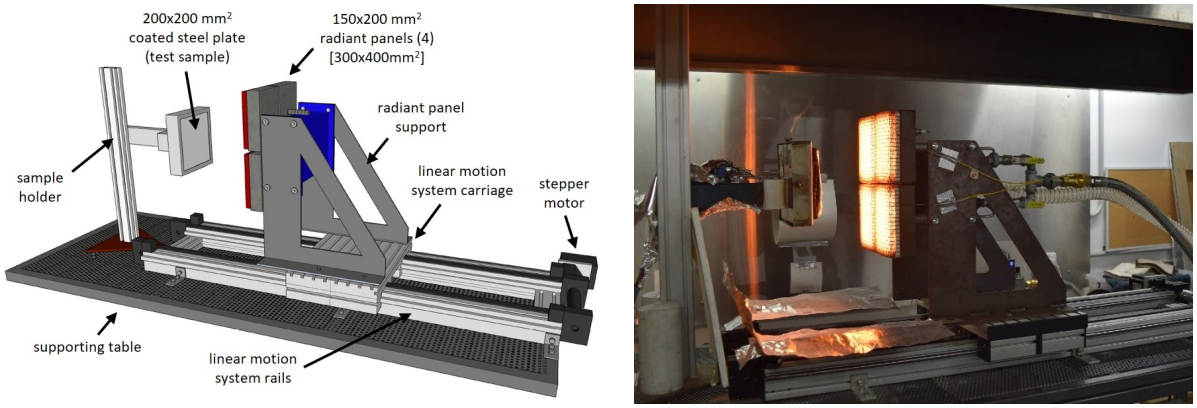

Fig. 1. Illustration of the experimental setup based on the H-TRIS test method.

defined time-history of incident radiant heat flux on the exposed surface of the test sample. In addition, thanks to its open environment, H-TRIS allows for the visual inspection of the test samples during the heating exposure (e.g. measuring the swelled coating thickness). The H-TRIS assembled for this specific research study was composed of four high-performance natural-gas-fired radiant panels mounted on a supporting frame and creating a 300 x 400 mm^2 radiant source of heat (Fig. 1). In this configuration, the apparatus can impose a wide range of incident radiant heat fluxes included between 5 and 100 kW/m^2 [19].

2.2 Test samples and description of the experiments

The samples used in this experimental study are 200 x 200 mm^2, 10 mm thick mild carbon steel plates, resulting in a section factor A_p/V (i.e. ratio between exposed surface and volume of steel) equal to 100 m^{-1} (Fig. 1). Based on the assembled H-TRIS, the sample dimensions were chosen in order to achieve a surface distribution of incident radiant heat flux on the sample surface with a deviation lower than 10%. The steel plates were professionally coated with a solvent-based thin intumescent coating. The product is commercialised worldwide for providing up to 120 minutes fire resistance to universal steel sections and cellular beams. It is commonly used in the built environment for internal, semi-exposed or external use and it is suitable for off-site and on-site application. The coating is a fast-track and self-priming coating, therefore it was applied in one hand using airless spray equipment, without the use of any primer or topcoat. After one month of curing, the applied DFT was measured using a non-destructive film thickness gauge at five different locations (at each corner and the centre of each coated plate). Based on the mean DFT measured over the steel plate surface, the test samples were selected to be categorised into three groups:

- *"Low DFT"* – 1.00 mm (± 0.20 mm)
- *"Medium DFT"* – 1.80 mm (± 0.20 mm)
- *"High DFT"* – 2.90 mm (± 0.20 mm)

Using the H-TRIS test method, coated samples were individually tested for 60 minutes under different levels of constant incident radiant heat flux: 10, 25, 40, 50, 70 and 90 kW/m^2 (Table 1). The heating conditions were explicitly chosen in order to subject the intumescent coating to various ranges of temperatures and heating rates, triggering the swelling reaction in different ways. Particularly, based on a previous research study, a constant incident radiant heat flux of 10 kW/m^2 was expected not to initiate the swelling process of the intumescent coating [15]. During the heating exposure, a custom-built steel frame was used in order to hold the test sample aligned with the inirepeatable thermal boundary conditions, heat losses at the back of the test sample were minimised by insulating the unexposed surface of test samples using a layer of 20 mm thick ceramic wool (ISOLITE ISOWOOL blanket) and 13 mm thick plasterboard (Knauf FireShield).

2.3 Instrumentation

The experimental setup was instrumented in order to systematically gauge all the possible information necessary to describe the thermo-physical response of the intumescent coating during the heating exposure.

1) The *thickness of the swelled intumescent coating* was measured by image processing of video footages taken using a high-resolution camera placed at the side of the test sample, aligned with

the surface of the test sample (Fig. 2). The swelled coating thickness was estimated in correspondence of the central area of test samples, therefore disregarding edge effects at the sample boundaries. The real-time measurement of the coating thickness was also used for continuously adjusting the relative distance between the intumescent coating surface and the array of radiant panels. In this way, the incident radiant heat flux at the exposed surface of the test sample was maintained to the specified value during the full duration of experiments.

2) Up to seven K-type thermocouples (1.5 mm diameter) were installed in the test sample in order to measure the *transient temperature profile within the intumescent coating*. Prior to testing, 1.8 mm holes were drilled through the steel plate in order to allow the insertion of the in-depth thermocouples from the rear of the test sample (Fig. 2). Preliminary tests evidenced that, if the thermocouples were placed at the beginning of the heating exposure, they would have perturbed the swelling process and the development of the intumescent char. Therefore, the thermocouples were inserted at specific locations within the swelling coating during the heating exposure. The real-time measurement of the swelled coating thickness was used to understand when a thermocouple could be inserted at a certain depth. The thermocouples were positioned at depths multiple of 5 mm from the interface between the coating and the steel plate: 5, 10, 15, 20, 25, 30, 35 mm. Particular care was taken in order not to damage the surface crust developed by the intumescent coating, which represents a key feature for the development of an effective thermal barrier [14].

3) The *temperature of the steel plate* was measured using up to three K-type thermocouples attached to the unexposed surface of the test samples (Fig. 2).

4) The *exposed surface temperature of the intumescent coating* was measured using an Infra-Red camera (model FLIR SC655: 16-bit 640 x 480 pixel resolution at 50 Hz, spectral range 7.5 - 14 µm, temperature range up to 2000 °C) (Fig. 2).

Table 1. Test matrix.

Sample group	Heating conditions	Number of repetitions	DFT_{mean} [mm]
"Low DFT"	10 kW/m^2	1	0.887
	25 kW/m^2	2	1.062, 1.204
	40 kW/m^2	2	0.996, 1.069
	50 kW/m^2	2	1.194, 1.196
	70 kW/m^2	2	1.162, 1.198
	90 kW/m^2	3	1.134, 1.146, 1.146
"Medium DFT"	10 kW/m^2	2	1.620, 1.712
	25 kW/m^2	2	1.638, 1.786
	40 kW/m^2	2	1.680, 1.816
	50 kW/m^2	3	1.794, 1.920, 2.014
	70 kW/m^2	2	1.712, 1.898
	90 kW/m^2	3	1.630, 1.770, 1.870
"High DFT"	10 kW/m^2	1	2.716
	25 kW/m^2	2	2.714, 2.902
	40 kW/m^2	2	2.750, 2.822
	50 kW/m^2	2	2.854, 2.866
	70 kW/m^2	2	2.878, 2.954
	90 kW/m^2	3	2.992, 3.038, 3.086

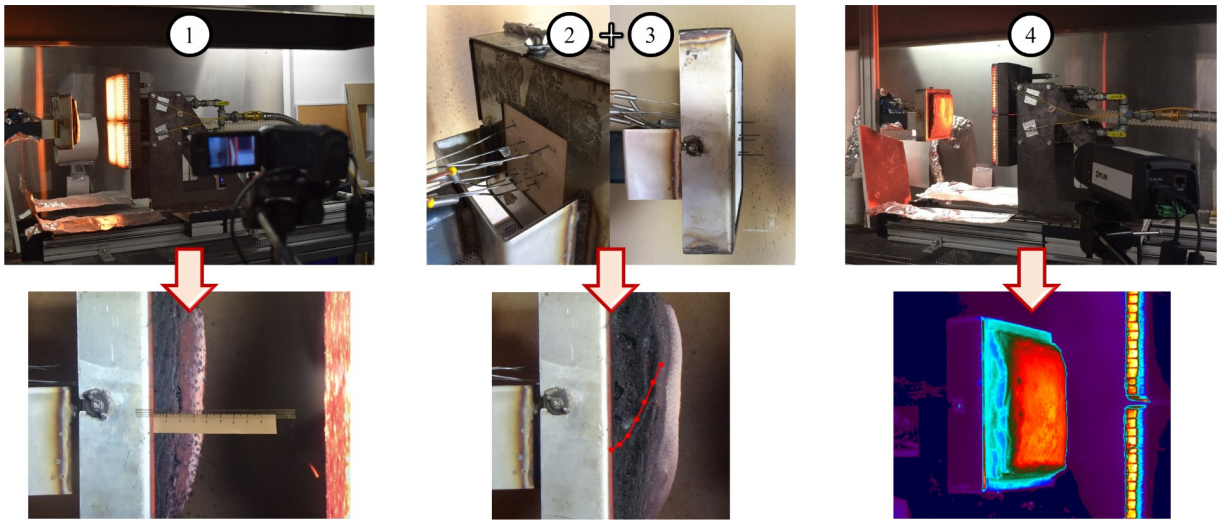

Fig. 2. Different aspects of the experimental setup designed to gauge the thermo-physical response of intumescent coatings during heating exposure.

2.4 Thermo-Gravimetric Analysis (TGA)

Aside from the experiments using H-TRIS, Thermo-Gravimetric Analysis (TGA) was performed on small powder samples of dry intumescent coating (8-10 mg) in order to study the thermal decomposition of the intumescent coating and understand at which temperature ranges the different reactions occur, particularly the intumescent swelling reaction. The TGA experiments were carried out using a PerkinElmer STA 6000. The intumescent coating was tested under different heating rates (5, 10, 20 and 30 °C/min) under N_2 or air in the temperature range 30-900 °C.

3 Experimental results

3.1 TGA results

Fig. 3 presents the results obtained from the TGA experiments in terms of normalised mass and its derivative (DTG curve). According to the available literature, the TGA results highlights that the product tested in this experimental study has similar characteristics to typical intumescent formulations. For instance, the common intumescent formulations are typically composed of a combination of ammonium polyphosphate (APP) as carbonisation catalyst, pentaerythritol (PER) as carbonisation agent, melamine (MEL) as blowing agent and acrylic resin as carbonic agent and binder. In these typical formulations, the carbonisation catalyst and agent transform their crystalline structure and melt at temperatures between 200 and 300°C, increasing the coating viscosity and releasing volatiles. The first peak in the DTG curves denotes this process, usually specified as *"Thermal Decomposition Zone"* or *"Melting Zone"*. The further decomposition and interaction of the different chemical compounds lead to the formation of the porous char structure by esterification: the blowing agent is activated and it releases large quantities of gases, which are trapped within the molten coating. The second peak in the DTG curves denotes this process, usually specified as *"Reaction Zone"* or *"Swelling Zone"* at temperatures between 300 and 400°C. The single reactions of the different compounds are often difficult to outline because of the synergic effect of blowing agent, carbonization catalyst and agent due to their similar decomposition and

reaction temperatures. In the two different atmospheres and under different heating rates, the main reactions occur at similar temperature ranges (200-400°C). These reactions are typically endothermic. Additionally, an oxidising atmosphere results in reactions shifting towards lower temperatures with a lower reaction rate compared to a reducing atmosphere. Another difference arises when the char gradually oxidises at temperatures higher than 600°C: the porous char structure degrades and CO_2 is released. This aspect is emphasised in the TGA results in air atmosphere: a first reaction was detected at about 650°C and a second reaction at about 800°C. The oxidation reactions are exothermic and they produce minor mass loss (lower than 5% each) [10, 23, 24].

In general, it is important to underline that the intumescent swelling reaction (second DTG peak) typically occurs at temperatures between 350 and 400°C and the main reactions of the intumescent coating can be considered to be completed at about 400 °C. At that temperature the main decomposing and swelling reactions are completed: the majority of the mass has been lost (about 40%), seeing the significant amount of inorganic compounds (about 40-45%).

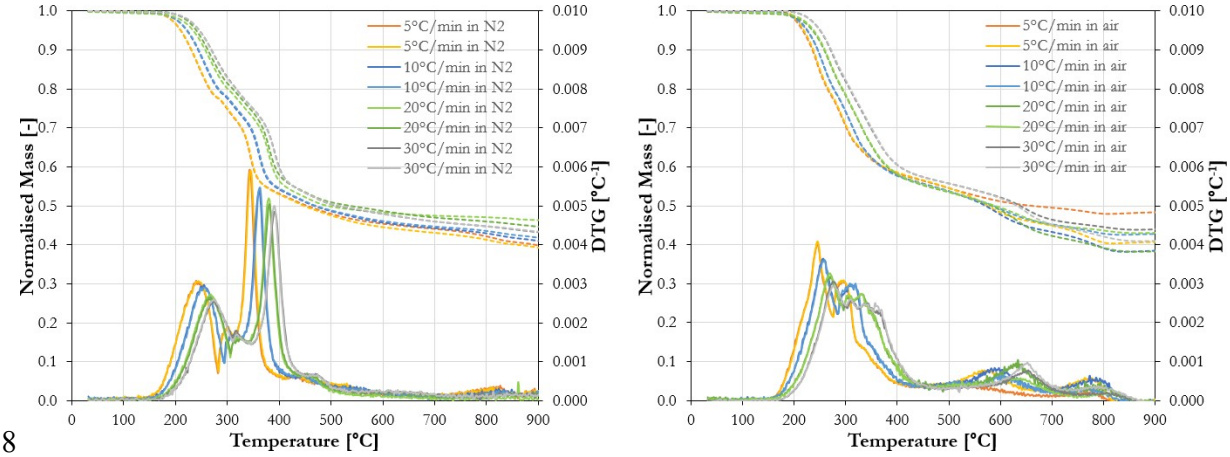

Fig. 3. TGA results in nitrogen (left) and air (right) atmospheres.

3.2 Steel temperatures and swelled coating thicknesses

Regarding the results obtained from the H-TRIS experiments, the performance of intumescent coatings was firstly characterised according to the evolution of the steel temperatures and the swelled coating thicknesses during the thermal exposure. Fig. 4 shows the evolution of the steel temperatures and the swelled coating thicknesses for all the different experiments carried out on coated samples. The good repeatability between experiments was confirmed by the agreement of the temperature readings and the estimations of the swelled coating thickness. Throughout all the experiments, the steel temperatures measured using thermocouples had deviations lower than 10%, the central area of the test samples swelled rather homogeneously and the swelled coating thicknesses were measured with an accuracy of ± 2 mm. For simplicity and neatness of graphical visualisation, only the average values are displayed in this manuscript. In the graphs, the same colour collects all the experiments with the same heating conditions, while continuous, dashed and dotted lines reports single experimental repetitions.

As regards the steel temperatures, most of the coated steel plates reached a steady-state temperature by the end of the heating exposure. However, in a few cases, the steel never reached a quasi-steady state temperature and the temperature kept increasing during the heating exposure, such as 50, 70

and 90 kW/m^2 for *"Low DFT"* and 70 and 90 kW/m^2 for *"Medium DFT"*. This aspect can be directly associated with the completion of the swelling process of the intumescent coating: in these cases, the coating completed the swelling process before the end of the experiment. In other cases, where the coating continuously swelled during the experiments, the steel plates tended to a similar range of steady-state temperatures, included between 300 and 350°C. The external incident heat flux had a minor influence. On the other hand, a higher applied initial DFT foreseeably produced a lower steady-state steel temperature due to the thicker porous char.

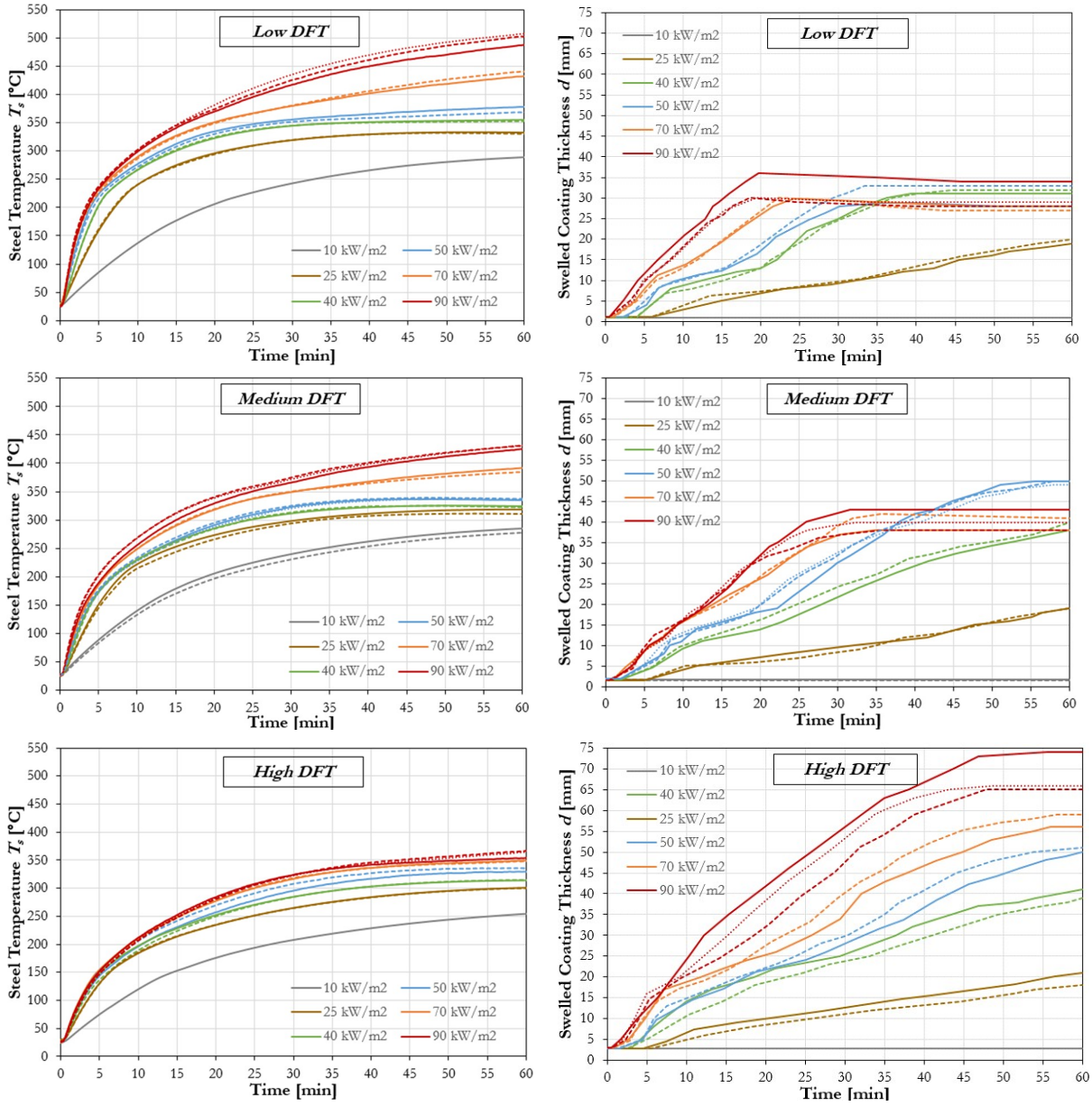

Fig. 4. Comparison of the evolution of the coated steel temperatures and the swelled coating thicknesses for the different applied initial DFTs and different constant incident heat fluxes.

With regards to the swelled coating thicknesses, right after the application of the incident heat flux, the intumescent coating quickly started swelling with different rates depending on the heating

conditions, i.e. the slope/derivative of the thickness-time curve (Fig. 4). As expected, the samples exposed to 10 kW/m^2 did not practically swell, regardless of the applied initial DFT. For the higher heat fluxes, the swelling rate of the intumescent coating appeared to be directly influenced by the external incident heat flux, while independent on the applied initial DFT. On the contrary, the applied initial DFT governed the maximum thickness that the coating could have reachedd during the thermal exposure. In particular, test samples coated with *"Low DFT"*, *"Medium DFT"* and *"High DFT"* swelled up to about 30 mm, 40 mm and 65 mm, respectively. Fig. 5 shows thetypical porous chars developed by the intumescent coating at the end of the thermal exposure: as shown in Fig. 4, a thicker intumescent porous char was produced for a higher constant incident heat flux. In order to emphasise the difference between different heating conditions, Fig. 5 reports the test samples coated with *"High DFT"*: in this case, the intumescent coating was able to swell throughout the whole duration of the heating exposure and develop the thickest porous chars (within the limits of this experimental study). For high heat fluxes, Fig. 5 also highlights the oxidation reactions occurring at the surface of the intumescent coating: the char turned into ash at the coating surface crust, characterised by a white/grey colour. This phenomenon can be clearly observed for constant incident heat fluxes of 70 and 90 kW/m^2, partially for 50 kW/m^2. Fig. 5 also shows that typical porous chars formed into a dome-like shape, in some cases (40 kW/m^2) more than others. However, the char shape had a minor influence on the experimental outcomes of this research study because all the temperature and swelling measurements were concentrated in the central area of the test sample, where even temperature and homogenous swelling were observed. In addition, the one-dimensional heat transfer was ensured due to the small view factor of the sample edges compared to the exposed surface of the intumescent coating.

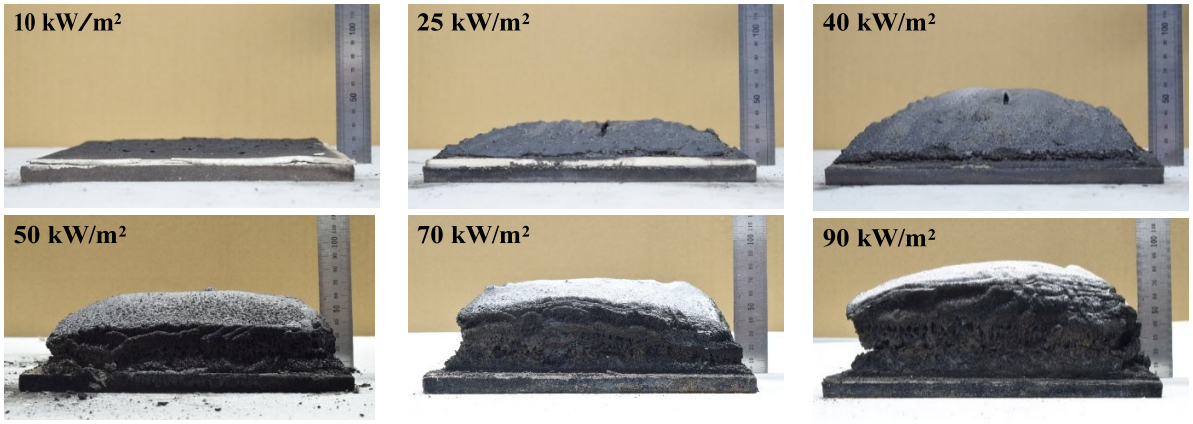

Fig. 5. Typical porous chars developed by the intumescent coating at the end of the thermal exposure for different constant incident heat flux (*"High DFT"*).

3.3 Surface coating temperature

In a post-test analysis, the temperature evolution at the exposed surface of the intumescent coating was evaluated by processing the data obtained by the Infra-Red camera. The coating emissivity value was set equal to 0.90 and the coating temperature was averaged over a 50 x 50 mm^2 area, placed at the centre of the test sample. The emissivity value has a key role in this process and it can significantly influence the results. Consequently, a sensitivity analysis of the surface emissivity value of the intumescent coating was performed: the same procedure was repeated for varying coating emissivity 0.90±0.05, accordingly to the average values found in a previous research study

(spectral range 2 - 20 µm) [15]. Fig. 6 shows the envelopes of the measured temperatures at the coating surface in all the experiments carried out under different heating conditions and applied initial DFTs. The continuous lines report the average temperatures calculated with an emissivity equal to 0.90, while the dotted lines define the envelopes obtained from the sensitivity analysis (maximum values: $\varepsilon = 0.85$; minimum values: $\varepsilon = 0.95$).

During the different experiments, the coating behaved like a low thermal inertia material by quickly reaching a specific surface temperature depending on the external heat flux and keeping a quasi-constant temperature during the rest of the heating exposure (thermally thick material characterised by a high Biot number). As expected, higher coating surface temperatures were measured for higher external constant incident heat fluxes. The applied initial DFT did not significantly influence the evolution of the coating surface temperature. In the second part of the heating exposure, the measured temperature gradually decreased, particularly for higher heat fluxes. This aspect could be related to the reduction in the emissivity due to the oxidation of the coating surface, which can be visually assessed through the colour change (white/grey). Another reason could be related to the migration of the oxidation front within the intumescent porous char: once the oxidation reaction (exothermic) is completed, the surface temperature decreases. Without any doubt, the lower surface temperatures measured in the cases of 70 kW/m^2 and 90 kW/m^2 can be directly associated with oxidation processes taking place at the coating surface. For heat fluxes higher than 50 kW/m^2, the measured surface temperatures were above 700°C: at this temperature range, oxidation is expected. This aspect is confirmed by the TGA results in oxidising atmosphere and photographs of the intumescent porous chars (Fig. 5), but it certainly needs further investigation to clarify the effects of the surface oxidation on the emissivity of swelling intumescent coatings.

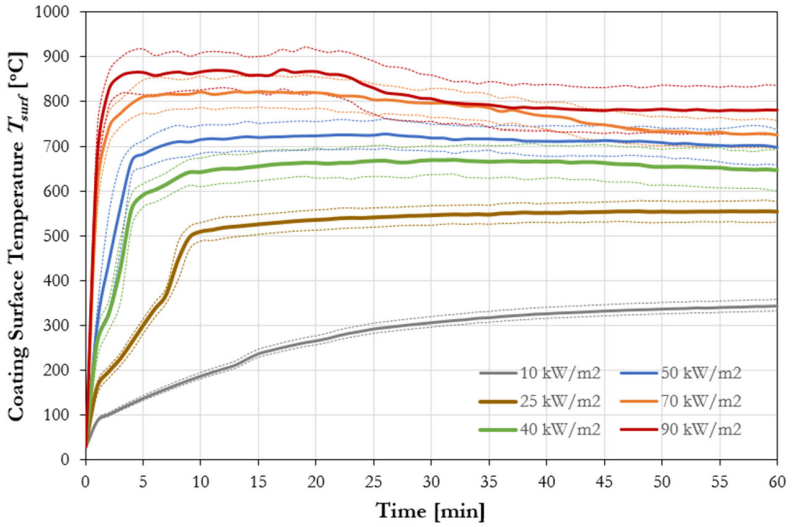

Fig. 6. Envelopes of the temperature evolution at the coating surface for the different external constant incident heat fluxes (all experiments with different applied initial DFTs are included).

3.4 Temperature profiles within the swelling coating

The heat transfer within swelling intumescent coatings was then investigated analysing the evolution of the in-depth temperature profiles. First, the agreement of the temperature readings between different experimental repetitions confirmed the good repeatability. In addition, theresults

highlighted the success of the designed experimental methodology able to accurately gauge the

thermo-physical response of intumescent coatings. Comparisons between experiments with and without in-depth thermocouples also confirmed the minor interference of the installed instrumentation. Fig. 7 shows the temperature profiles measured at the end of the heating exposure for all the different experiments on coated samples. The temperature profiles can be assumed as steady-state if the swelling process of the intumescent coating was completed. The in-depth temperatures at different depths within the intumescent coating are reported with the average surface temperatures ($\varepsilon = 0.90$). For visualisation purposes, the error bars were omitted from the graphs. However, the in-depth thermocouples were placed within the intumescent coating with an accuracy ±2 mm and the measured in-depth temperatures had a deviation lower than 10%. The steady-state temperature profiles shown in Fig. 7 had similar thermal gradients (slope of the in-depth temperature profile) within the intumescent coating. This aspect suggested that the intumescent porous char had similar thermal and physical properties, regardless of the imposed heating conditions. As already explained in the previous section, after the first transient period, the coating surface temperature can be considered as constant and it can be directly related to the external constant incident heat flux. Regarding the steel substrate, if the coating underwent continuous swelling, the steel temperature remained within a similar range (300-350°C). Consequently, the thermal gradient with the intumescent coating was governed by the swelled coating thickness. Since the extremes of the intumescent coating can be considered to have a quasi-constant temperature, further swelling resulted in stretching the thermal gradient between the steel substrate and the coating surface. This aspect is highlighted in Fig. 9: at 50 kW/m^2, a steel plate coated with *"High DFT"* continuously swelled during the heating exposure and the steel temperature did not overcome 350°C. On the other hand, at 50 kW/m^2, a steel plate coated with *"Low DFT"* completed the swelling reaction after about 30-35 minutes of heating exposure and, beginning from that moment, the steel temperature started increasing above 350°C.

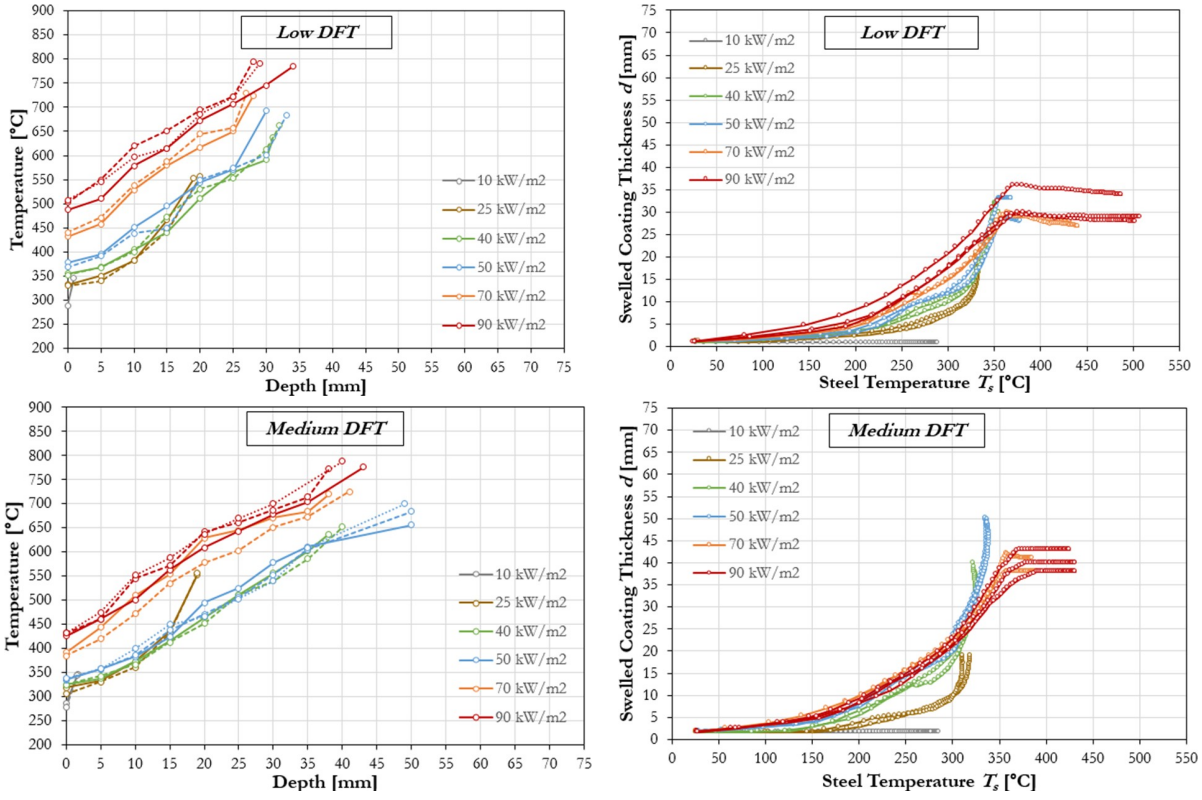

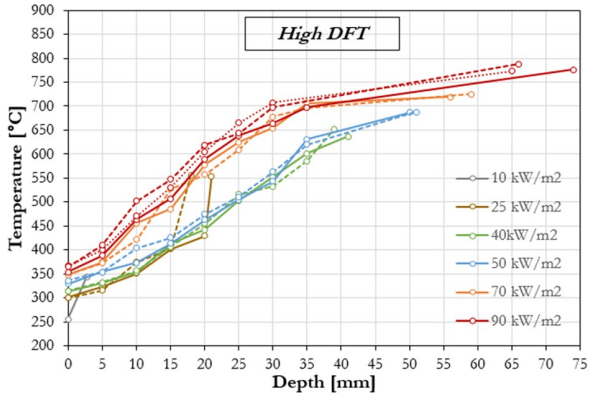

Fig. 7. Comparison of the measured temperature profiles at the end of the heating exposure for different applied initial DFTs and different constant incident heat fluxes.

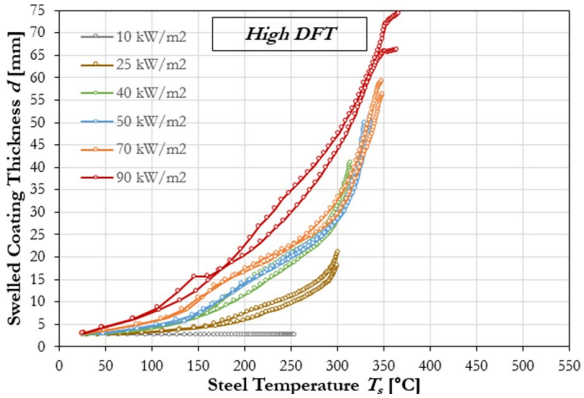

Fig. 8. Swelled coating thicknesses as a function of the coated steel temperature for different applied initial DFTs and different constant incident heat fluxes.

333

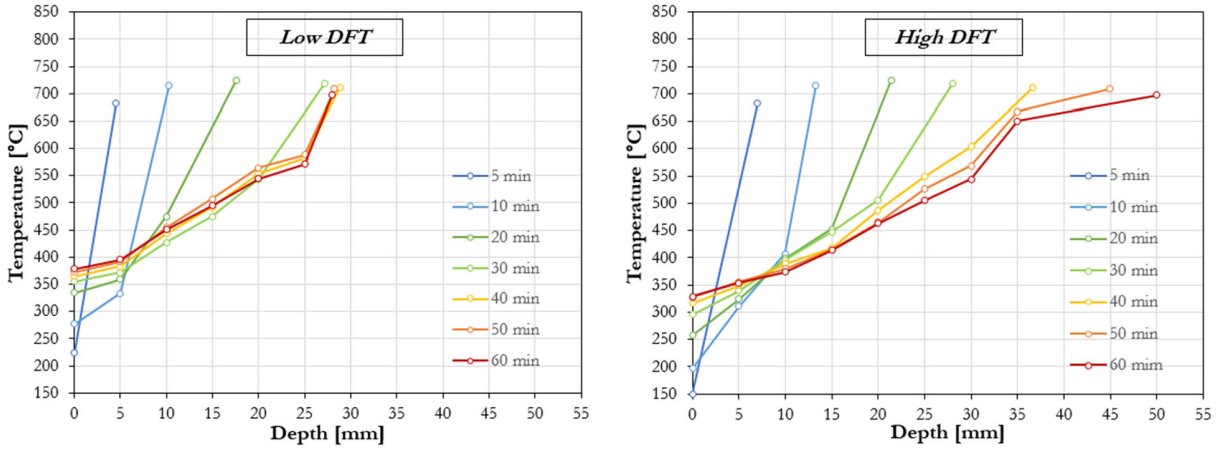

334

335 Fig. 9. Comparison of the evolution of the temperature profiles (in-depth and surface) at different
336 instants during the heating exposure with different applied initial DFTs exposed to 50 kW/m^2.

337 4 Analysis and discussion

338 So far, the experimental investigation has underlined how the evolutions of the steel temperature
339 and the swelled coating thickness are closely related and they have key roles in the understanding
340 and the assessment of the effectiveness of intumescent coatings. Fig. 8 reports the evolution of the
341 swelled coating thicknesses as a function of the coated steel temperature for different applied initial
342 DFTs and heating conditions. The experimental results confirmed how, in case of continuous
343 swelling, the coated steel plates asymptotically tended to a similar temperature range included
344 between 300 and 350°C, regardless of the heating condition or the applied initial DFT. Contrarily,
345 when the coating completed the swelling process, the steel temperatures increased above this
346 threshold. This aspect is supported by the results obtained by TGA: the intumescent swelling
347 reaction occurs at temperatures between 350 and 400°C and it can be considered to be completed
348 at about 400 °C.

The evolution of coated steel temperatures provides a first assessment of the coating effectiveness: i.e. the colder the steel, the better thermal insulation. In turn, as shown in Fig. 8, the coated steel temperatures can be directly linked to the coating swelling process. Therefore, it can be concluded that the swelling process and the resulting swelled thickness govern the thermo-physical response of intumescent coatings, thus their effectiveness. In particular, the coated steel temperature acts as an indicator of the swelling process of intumescent coatings: if the steel temperature overcomes 350°C, the swelling reaction is completed. This aspect has been verified also by a close investigation of the recorded video footage. This experimental outcome suggests that the swelling reaction takes place close to the steel substrate: particularly, about the interface between the steel and the applied intumescent coating. The intumescent coating swells and insulates the steel substrate by displacing the already-swelled coating towards the direction of the source of heat. The swelling reaction continues at the virgin coating located behind the swelled porous char and in the proximity to the steel substrate. This process lasts until the intumescent coating is fully consumed, which can be directly related to the applied initial DFT. As a conclusion, the steel temperature can be directly associated with the swelling process because it defines the temperature experienced by the virgin coating, which is located behind the swelled porous char and sustains the swelling reaction [25].

The non-unique relationship between the steel temperature and the swelled coating thickness shown in Fig. 8 may be explained by the direct influence of the heating conditions. In particular, experimental results highlighted that higher external incident heat fluxes produced higher coating thicknesses while the steel remains at the same temperature. Assuming similar thermal and physical properties of the intumescent porous char (as discussed in section 3.4), a higher net heat flux to the virgin coating, which sustains the swelling reaction, is expected. Consequently, a higher incident heat flux at the coating surface provides higher net heat flux to the swelling reaction, thus it governs the swelling rate. For instance, an incident heat flux of 10 kW/m^2 did not trigger the swelling reaction due to the low steel temperatures (below 300°C) and the low net heat flux received by the virgin coating.

Nevertheless, the experimental study presented herein emphasised how the swelling process and the resulting swelled thickness govern the thermo-physical response of intumescent coatings, thus their effectiveness. In particular, the influence of heating conditions and the applied initial DFT can be clearly outlined and empirical correlations can be derived. First, the applied initial DFT governs the maximum swelled thickness that the intumescent coating could have reached during the thermal exposure. The applied initial DFT provides a quantification of the intumescent material that can potentially swell and hence produces porous char. Fig. 10 defines a possible linear correlation between the applied initial DFT and the maximum swelled thickness of the intumescent coating after the completion of the swelling process. Regarding the heating conditions, the external incident heat flux at the coating surface governs the swelling rate of intumescent coatings. Fig. 11 defines a possible linear correlation between the constant incident heat flux and the swelling rate of the intumescent coating. In this calculation, the swelling rate of the intumescent coating was linearised from the onset of swelling until the instant when the maximum swelled thickness was reached. Theoretically, it should be possible to correlate the swelling rate to more fundamental parameters, such as the net flux through the swelled porous char and received by the virgin coating that sustains the swelling reaction. The process would be possible only by formulating a heat transfer model. However, the thermal and physical properties of intumescent porous chars should be defined in order to estimate such parameters. This aspect is outside the scope of the current

manuscript, but future studies will focus on that. As a conclusion, this experimental investigation presented how the swelling of intumescent coatings, which is the main factor that governs their thermos-physical response and their effectiveness, can be predicted starting from well-defined thermal boundary conditions at the coating surface and applied initial DFT.

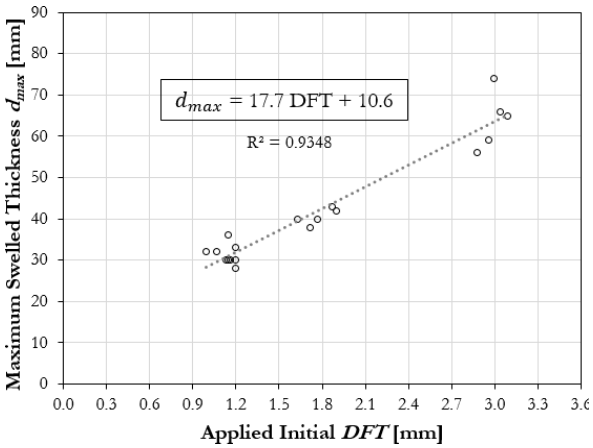

Fig. 10. Relationship between the applied initial DFT and the maximum swelled thickness of the intumescent coating.

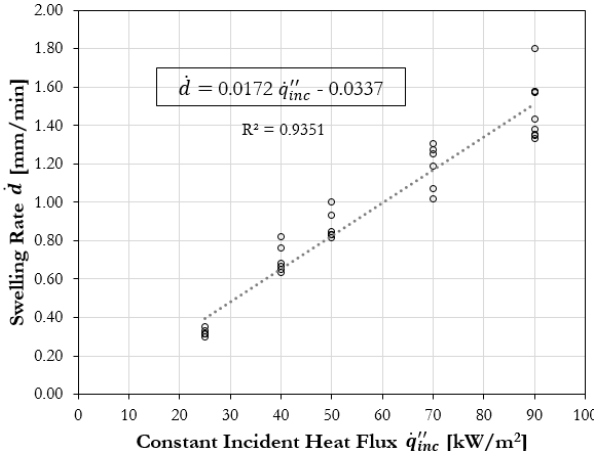

Fig. 11. Relationship between the external constant incident heat flux and the swelling rate of the intumescent coating.

5 Conclusions

The current practice of designing steel structures protected with intumescent coatings offers simplified engineering methods able to simulate the temperature evolution of coated steel samples tested in furnaces and exposed a single heating scenario. However, in a world moving towards performance-based solutions, there is a need for explicitly understanding how different factors may influence the effectiveness of intumescent coatings. The study presented herein shows an experimental methodology aimed at analysing the effectiveness of intumescent coatings through a detailed characterisation of their thermo-physical response for a range of heating conditions and applied initial dry film thickness (DFT). Steel plates coated with a commercial solvent-based thin intumescent coating were exposed to well-defined and highly-repeatable heating conditions using radiant panels and in accordance with the Heat-Transfer Rate Inducing System (H-TRIS) test method. Experimental results demonstrate high repeatability between experiments and the ability to measure real-time swelled coating thickness, the exposed surface temperature, the steel temperature and the in-depth transient temperature profile within the intumescent coating. From the experimental results, the following concluding remarks may be drawn:

- The swelling process and the resulting swelled thickness govern the thermo-physical response of intumescent coatings, thus their effectiveness. During swelling, the temperature of coated steel plates asymptotically tends to a temperature range between 300 and 350°C, regardless of the heating condition or the applied initial DFT. When the coating completes its swelling process, the steel temperature increases above 350°C. This aspect is supported by the material characterisation obtained by TGA experiments: the swelling reaction occurs at temperatures between 350 and 400°C and it can be considered to be completed at about 400 °C.

- The swelling reaction occurs in the proximity to the steel-coating interface. The intumescent coating swells and insulates the steel substrate by displacing the already-swelled coating towards the direction of the source of heat. This explains why coated steel temperature acts as an indicator of the swelling process of intumescent coatings.
- The measured in-depth temperature profiles within the swelling coating suggest that the intumescent porous char has similar thermal and physical properties, regardless of the heating conditions or the applied initial DFT. The thermal gradient within the intumescent coating is governed by the swelled coating thickness.
- The heating conditions and the initial thickness differently influence the swelling process of intumescent coatings: the applied initial DFT governs the maximum swelled thickness, while the external incident heat flux at the coating surface governs the swelling rate. Using the empirical correlations derived based on the experimental results, the swelling of the tested intumescent coating can be predicted.

Future studies should focus on quantifying the thermal and physical properties of the intumescent porous char and implementing heat transfer models able to simulate the response of intumescent coatings. In particular, it would be interesting to understand if the net heat flux to the virgin coating, which is located behind the swelled porous char and sustains the swelling reaction, may be correlated to the swelling rate. Finally, the authors believe that the product tested in this experimental study represents a common behaviour of typical thin intumescent coatings commercially available in the market. However, other products with different formulations should be investigated before generalising research outcomes.

Acknowledgements

The authors are grateful for the support of Remedial Building Services Australia Pty Ltd, in particular Qazi Samia Razzaque, Edward Kwok, Long Le and Andrew Abrahams. The authors would like also to gratefully acknowledge the Fire Safety Engineering Research Group at The University of Queensland, in particular Jeronimo Carrascal Tirado, for the continuous inspiration, feedback and technical support. The authors would also like to thank the financial support from the Faculty of Engineering, Architecture and Information Technology at The University of Queensland, partially funding this research with a Philanthropic Grant for Early Career Engineering.

References

[1] Usmani A.S., Rotter J.M., Lamont S., Sanad A.M. and Gillie M. "Fundamental principles of structural behaviour under thermal effects". Fire Safety Journal, vol. 36, pp. 721-744, 2001.

[2] Buchanan A.H. and Abu A.K. "Structural design for fire safety". John Wiley & Sons, 2nd Edition, 2017.

[3] Mariappan T. "Recent developments of intumescent fire protection coatings for structural steel: A review". Journal of Fire Sciences, vol. 34, no. 2, pp. 1-44, 2016.

[4] Weil E.D. "Fire-protective and flame-retardant coatings – A state-of-the-arte review". Journal of Fire Science, vol. 29, pp.259-296, 2011.

[5] Puri E.G., Khanna A.S. "Intumescent coatings: a review on recent progress". Journal of Coatings Technology and Research, vol. 14, pp. 1-20, 2017.

[6] Elliott A., Temple A., Maluk C. and Bisby L. "Novel testing to study the performance of intumescent coatings under non-standard heating regimes". Fire Safety Science – Proceedings of the 11th International Symposium, University of Canterbury, New Zealand, pp.652-665, 2014.

[7] Taylor A.P. and Sall F.R. “Thermal analysis of intumescent coatings”. European Polymer Paint Colour Journal, vol. 182, no. 4301, pp. 122-130, 1992.
[8] International Organization for Standardization (ISO). “ISO834-1:1999 Fire resistance tests - Elements of building construction - Part 1: General requirements for fire resistance testing”. Geneva, Switzerland, 1999.
[9] Comité Europeén de Normalization (CEN). “EN 13381-8:2013 Test methods for determining the contribution to the fire resistance of structural members - Part 8: Applied reactive protection to steel members”. Brussels, Belgium, 2013.
[10] Lucherini A. and Maluk C. “Intumescent coatings used for the fire-safe design of steel structures: A review”. Journal of Constructional Steel Research, vol. 162, n. 105712, 2019.
[11] Li G.Q., Lou G.B., Zhang C., Wang L. and Wang Y. "Assess the fire resistance of intumescent coatings by equivalent constant thermal resistance". Fire Technology, vol. 48, pp. 529-546, 2012.
[12] Wang L., Dong Y., Zhang D., Zhang D. and Zhang C. "Experimental study of heat transfer in intumescent coatings exposed to non-standard furnace curves". Fire Technology, vol. 51, no. 1, pp. 627-643, 2015.
[13] Zhang Y., Wang Y., Bailey C.G. and Taylor A.P. "Global modelling of fire protection performances of an intumescent coating under different furnace re conditions". Journal of Fire Science, vol. 31, no.1, pp. 51-72, 2012.
[14] Lucherini A., Giuliani L. and Jomaas G. “Experimental study of the performance of intumescent coatings exposed to standard and non-standard fire conditions”. Fire Safety Journal, vol. 95, pp. 42-50, 2018.
[15] Lucherini A. and Maluk C. “Assessing the onset of swelling for thin intumescent coatings under a range of heating conditions”. Fire Safety Journal, vol. 106, pp. 1-12, 2019.
[16] de Silva D., Bilotta A and Nigro E. “Experimental investigation on steel elements protected with intumescent coating”. Construction and Building Materials, vol. 205, pp. 232-244, 2019.
[17] Maluk C., Bisby L., Terrasi G., Krajcovic M., Torero J.L. “Novel fire testing methodology: why, how and what now?”. Proceedings of the Mini Symposium on Performance-based Fire Safety Engineering of Structures as part of the 1st International Conference on Performance Based land Life Cycle Structural Engineering, pp. 448-458, 2012.
[18] Maluk C., Bisby L., Krajcovic M. and Torero J.L. “A Heat-Transfer Inducing System (H-TRIS) Test Method”. Fire Safety Journal, vol. 105, pp. 307-319, 2019.
[19] Lucherini A. and Maluk C. “Novel test methods for studying the fire performance of thin intumescent coatings”. Proceedings of 2nd International Fire Safety Symposium (IFireSS), Napoli, Italy, pp. 565-572, 2017.
[20] Bozzoli F., Mocerino A., Ranieri S. and Vocale P. “Inverse heat transfer modeling applied to the estimation of the apparent thermal conductivity of an intumescent fire retardant paint”. Experimental Thermal and Fluid Science, vol. 90, pp. 143-152, 2018.
[21] Hsu S.Y. “Modeling of heat transfer in intumescent fire-retardant coating under high radiant heat source and parametric study on coating thermal response”. Journal of Heat Transfer, vol. 140, n. 3, 2017.
[22] Kang J., Takahashi F. and T’ien J.S. “In situ thermal-conductivity measurements and morphological characterization of intumescent coatings for fire protection”. Journal of Fire Sciences, vol. 36, n. 5, pp. 419-437, 2018.
[23] Wang Z., Han E. and Ke W. “Effects of nanoparticles on the improvement in fire-resistant and anti-ageing properties of flame-retardant coating”. Surface & Coatings Technology, vol. 200, pp. 5706-5716, 2006.
[24] Bourbigot S., Le Bras M., Duquesne S. and Rochery M. “Recent Advances for Intumescent Polymers”. Macromolecular Materials and Engineering, vol. 289, pp. 499–511, 2004.
[25] Lucherini A., Torero J.L. and Maluk C. “Effects of thermal conditions of steel on the fire performance of thin intumescent coatings. Proceedings of the 15th International Conference and Exhibition on Fire Science and Engineering (Interflam), Royal Holloway College, London, UK, 2019.

512 Figure captions

513 Fig. 1. Illustration of the experimental setup based on the H-TRIS test method.

514 Fig. 2. Different aspects of the experimental setup designed to gauge the thermo-physical response
515 of intumescent coatings during heating exposure.

516 Fig. 3. TGA results in nitrogen (left) and air (right) atmospheres.

517 Fig. 4. Comparison of the evolution of the coated steel temperatures and the swelled coating
518 thicknesses for the different applied initial DFTs and different constant incident heat fluxes.

519 Fig. 5. Typical porous chars developed by the intumescent coating at the end of the thermal
520 exposure for different constant incident heat flux (*"High DFT"*).

521 Fig. 6. Envelopes of the temperature evolution at the coating surface for the different external
522 constant incident heat fluxes (all experiments with different applied initial DFTs are included).

523 Fig. 7. Comparison of the measured temperature profiles at the end of the heating exposure for
524 different applied initial DFTs and different constant incident heat fluxes.

525 Fig. 8. Swelled coating thicknesses as a function of the coated steel temperature for different
526 applied initial DFTs and different constant incident heat fluxes.

527 Fig. 9. Comparison of the evolution of the temperature profiles (in-depth and surface) at different
528 instants during the heating exposure with different applied initial DFTs exposed to 50 kW/m^2.

529 Fig. 10. Relationship between the applied initial DFT and the maximum swelled thickness of the
530 intumescent coating.

531 Fig. 11. Relationship between the external constant incident heat flux and the swelling rate of the
532 intumescent coating.

533 Table captions

534 Table 1. Test matrix.